

Structure and magnetic properties of the two-dimensional antiferromagnet Na_2TbO_3

This article has been downloaded from IOPscience. Please scroll down to see the full text article.

2005 J. Phys.: Condens. Matter 17 4393

(<http://iopscience.iop.org/0953-8984/17/27/014>)

View [the table of contents for this issue](#), or go to the [journal homepage](#) for more

Download details:

IP Address: 129.252.86.83

The article was downloaded on 28/05/2010 at 05:14

Please note that [terms and conditions apply](#).

Structure and magnetic properties of the two-dimensional antiferromagnet Na_2TbO_3

Yoshihiro Doi¹, Kensuke Ninomiya¹, Yukio Hinatsu¹ and Kenji Ohoyama²

¹ Division of Chemistry, Graduate School of Science, Hokkaido University, Sapporo 060-0810, Japan

² Institute for Materials Research, Tohoku University, Sendai 980-8577, Japan

Received 13 April 2005, in final form 7 June 2005

Published 24 June 2005

Online at stacks.iop.org/JPhysCM/17/4393

Abstract

The crystal structure and magnetic properties of ternary oxide Na_2TbO_3 were investigated. This compound has a monoclinic structure with space group $C2/c$. The cations form two kinds of layers, one of which is composed of Na and O atoms, the other consisting of Na, Tb, and O atoms. In the latter, the Tb ions are arranged in a honeycomb manner. Powder x-ray and neutron diffraction measurements show that a partially disordered arrangement has been found between Na and Tb ions ($\sim 20\%$). A broad peak of the magnetic susceptibility against temperature was observed at ~ 60 K, which is due to a two-dimensional characteristic of the magnetic order of the Tb ions. At lower temperatures, this compound shows an antiferromagnetic transition at 38.3 K. The magnetic structure of Na_2TbO_3 was determined by powder neutron diffraction measurement at 2.6 K. The magnetic moments of the Tb^{4+} ions ($\sim 6 \mu_B$) order in the collinear antiferromagnetic arrangement.

1. Introduction

The oxides containing lanthanide (Ln) ions have been attracting interest since they often show anomalous magnetic properties at low temperatures. Recently, the pyrochlore oxides $\text{Ln}_2\text{Ti}_2\text{O}_7$ have been vigorously investigated. They have a corner-sharing tetrahedral array of Ln ions which brings about geometric frustration, and some of them (Ln = Ho and Dy) show a phenomenon called ‘spin ice’ [1, 2]. We believe that studying the oxides in which the Ln ions adopt peculiar arrays (linear, triangular, Kagomé, pyrochlore, fcc, etc) is a possible approach to finding new magnetic properties, because they are frustrated and/or low dimensional lattices [3–5].

The most stable oxidation state of lanthanide ions is trivalent, and their magnetic properties are determined by the unpaired 4f electrons. Generally, the shielding by outer 5s and 5p electrons surrounding the 4f electrons makes the magnetic interaction between Ln ions very weak. In fact, many lanthanide oxides order magnetically below 4 K [6]. However, among

oxides containing Ln ions in unusual oxidation states such as the divalent and tetravalent states, there are some compounds showing exceptionally high magnetic transition temperatures, for example Eu^{2+}O ($T_c = 70$ K) [7] and $\text{BaTb}^{4+}\text{O}_3$ ($T_N = 33.4$ K) [8].

Here, we focused our attention on the magnetic properties of ternary oxides $\text{Na}_2\text{Ln}^{4+}\text{O}_3$ (Ln = Pr, and Tb). These compounds adopt NaCl-related structures with some structural modifications [9–11], one of which is the cubic NaCl structure in which Na and Ln ions adopt a disordered arrangement in the cation sites; the other is the cation-ordered structure: for Na_2PrO_3 , Na and Pr ions are fully ordered in close-packing layers corresponding to the (111) plane of cubic NaCl structure, and for Na_2TbO_3 , the close-packing layers containing only Na ions and those containing ordered $(1/3)\text{Na}$ and $(2/3)\text{Tb}$ ions are alternately stacked. Among such modifications, Na_2TbO_3 is regarded as a two-dimensional (2D) magnet since the layers containing magnetic ions (Tb^{4+}) are magnetically separated by the nonmagnetic Na–O layers. Thus, $\text{Na}_2\text{Tb}^{4+}\text{O}_3$ may show interesting magnetic properties due to its two dimensional arrangement. In addition, we can expect to observe magnetic transitions at relatively high temperatures, because the Tb ions are in the tetravalent state.

Recently, we have reported the structure and magnetic properties of Na_2PrO_3 [12]. This compound has a new type of cation ordering structure. Its crystal structure is different from that reported previously [10] and is fairly similar to that for Na_2TbO_3 [10]. In addition, a disordered arrangement of Na and Pr ions has been observed. Na_2PrO_3 shows an antiferromagnetic transition at $T_N = 4.7$ K. The temperature dependence of the magnetic susceptibility suggests the occurrence of short range magnetic ordering at a higher temperature than T_N . On the other hand, the magnetic behaviour of Na_2TbO_3 is unknown, except for the magnetic susceptibility in the paramagnetic region [13].

In this paper, we have investigated the crystal structure and magnetic properties of Na_2TbO_3 by using powder x-ray and neutron diffraction, magnetic susceptibility, and specific heat measurements.

2. Experimental details

Two polycrystalline samples (Na_2CeO_3 and Na_2TbO_3) were prepared by solid-state reaction. The Na_2CeO_3 was needed to estimate the lattice and electronic contribution to the total specific heat for Na_2TbO_3 , which will be described later. The starting materials, lanthanide oxides (CeO_2 or Tb_4O_7) and 10% excess Na_2O_2 , were mixed using agate mortar in a glove box filled with argon gas. For Na_2TbO_3 , the mixtures were enclosed with a gold tube, and then it was sealed in an evacuated silica tube. In order to remove excess oxygen, Ti_2O_3 was put in the end portion of the silica tube. They were heated at 973 K for 12 h, and then at 1073 K for 2 h with an intermediate grinding. For Na_2CeO_3 , mixtures of the starting materials were enclosed with a gold tube, and heated at 973 K for 12 h in an atmosphere of O_2 gas.

The x-ray diffraction measurements were performed at room temperature in the range $10^\circ \leq 2\theta \leq 120^\circ$ using a 2θ step size of 0.02° with Cu $K\alpha$ radiation on a Rigaku MultiFlex diffractometer. Powder neutron diffraction profiles were measured for Na_2TbO_3 at 2.6, 50, and 290 K in the range $3^\circ \leq 2\theta \leq 153^\circ$ at intervals of 0.1° with the wavelength of 1.82035 Å. Measurements were performed by the Kinken powder diffractometer for high efficiency and high resolution measurements, HERMES, of the Institute for Materials Research (IMR), Tohoku University [14], installed at the JRR-3M reactor in the Japan Atomic Energy Research Institute (JAERI), Tokai. The x-ray and neutron diffraction data were analysed by the Rietveld technique, using the programs RIETAN2000 [15].

The temperature dependence of the magnetic susceptibilities was measured in both zero-field-cooled (ZFC) and field-cooled (FC) conditions in an applied field of 0.1 T over the

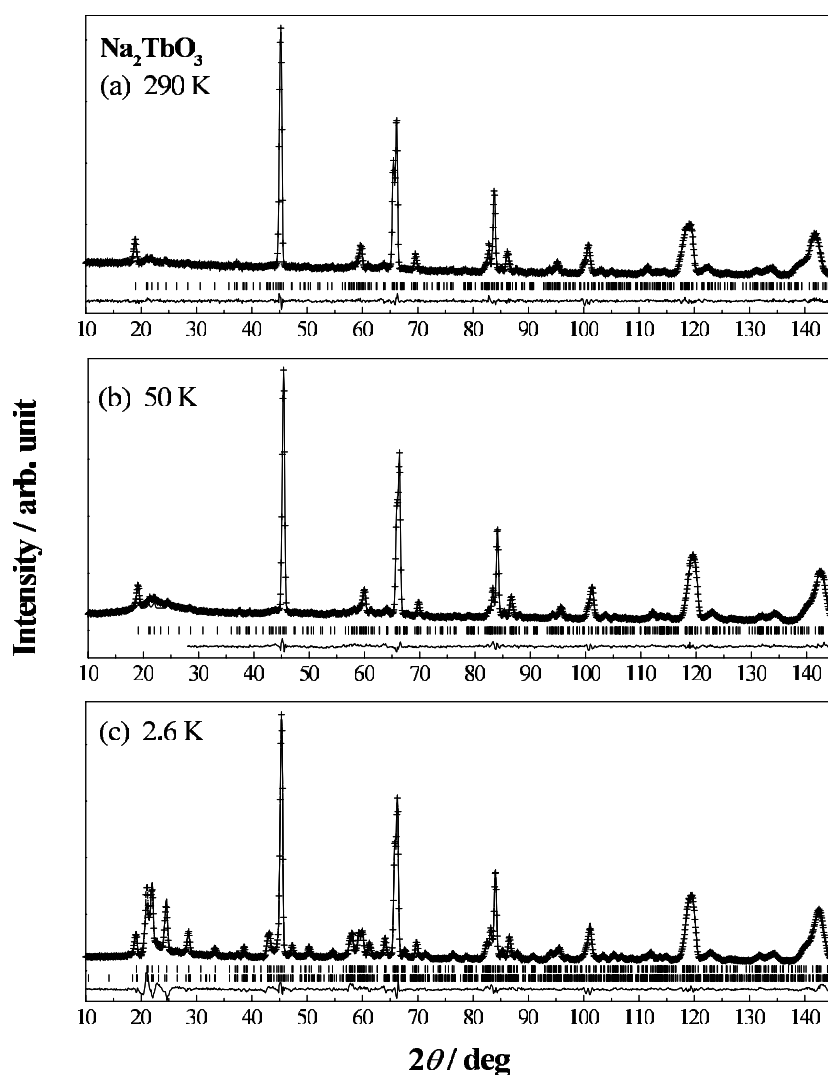


Figure 1. Powder neutron diffraction profiles for Na_2TbO_3 at 290 K (a), 50 K (b), and at 2.6 K (c). The vertical marks represent the peak positions for the nuclear reflections; in (c), those for magnetic reflections are added as lower vertical marks.

temperature range 1.8–400 K using a SQUID magnetometer (Quantum Design, MPMS-5S). Specific heat measurements were performed using a relaxation technique with a commercial physical property measurement system (Quantum Design, PPMS model) in the temperature range 1.8–300 K. The sintered sample in the form of a pellet was mounted on a thin alumina plate with grease for better thermal contact.

3. Results and discussion

3.1. Crystal structure

Figure 1(a) shows the powder neutron diffraction profile for Na_2TbO_3 at 290 K. The x-ray and neutron diffraction data were indexed with a monoclinic unit cell, space group $C2/c$.

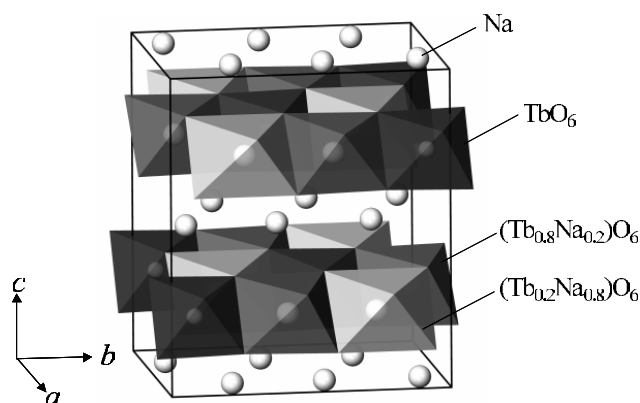


Figure 2. The crystal structure of Na_2TbO_3 .

According to the previous study [10], Na_2TbO_3 adopts a fully ordered structure consisting of the Na and $(\text{Na}_{1/3}\text{Tb}_{2/3})$ layers. In the Na layer, the suggested site positions for Na ions were 4d and 8f in $C2/c$, and in the $(\text{Na}_{1/3}\text{Tb}_{2/3})$ layer, three independent 4e site positions were suggested to be occupied by Na, Tb, and Tb ions, respectively. The Tb ions form a 2D honeycomb lattice in the latter layer. Initially, we attempted to analyse the data using this model; however, the intensities of the observed and calculated reflections showed poor matching in the low angle region. Thus, we assumed a disordered arrangement of Na and Tb ions in the three 4e sites. The Rietveld analysis showed that one of the three 4e sites is occupied only by Tb ions, and the other two 4e sites are occupied by both Na and Tb ions. In the latter case, they are partially ordered: one is occupied by Na (80%) and Tb (20%) and the other is occupied by Na (20%) and Tb (80%). The structural parameters determined by the neutron diffraction measurements are summarized in table 1. The crystal structure for Na_2TbO_3 is illustrated in figure 2. The x-ray diffraction profile for Na_2CeO_3 resembles that for Na_2TbO_3 . Rietveld analyses for Na_2CeO_3 show that this compound also adopts the partially ($\sim 35\%$) ordered structure. The refined structural parameters are shown in table 2.

Some bond lengths for Na_2TbO_3 calculated from the structural parameters are summarized in table 3. All the cations occupy the six-coordinated sites. The average M–O bond lengths for $M = \text{Na}1, \text{Na}2$, and $\text{Tb}3$ are in good agreement with lengths calculated from the Shannon's ionic radii [16]: $\text{Na}^+ - \text{O}^{2-}$ 2.42 Å, $\text{Tb}^{4+} - \text{O}^{2-}$ 2.16 Å, respectively. The average M–O lengths for disordered sites, 2.396(18) Å for $M = \text{Na}3/\text{Tb}1$ and 2.192(13) Å for $M = \text{Na}4/\text{Tb}2$, reflect the respective occupancies (table 1).

3.2. Magnetic susceptibility

The temperature dependence of the ZFC and FC magnetic susceptibility for Na_2TbO_3 is plotted in figure 3. The ZFC data in the higher temperature region ($T > 150$ K) were fitted by the Curie–Weiss law; the effective magnetic moment and Weiss constant were determined to be 7.90(8) μ_B and $-105(4)$ K, respectively. This magnetic moment is in good agreement with the free-ion value (7.94 μ_B) of the Tb^{4+} ion with $S = 7/2$. The negative Weiss constant suggests an antiferromagnetic interaction between Tb ions.

At lower temperatures, the deviation from the Curie–Weiss curve becomes larger and the magnetic susceptibility shows a broad maximum at 60 K. This behaviour may be due to the 2D nature of the magnetic interaction. If we ignore the 20% disorder of two 4e sites,

Table 1. Structural parameters for Na₂TbO₃ determined by the powder neutron diffraction measurement.

Atom	Site	<i>x</i>	<i>y</i>	<i>z</i>	<i>B</i> (Å ²)	Occupancy
<i>T</i> = 290 K						
Space group <i>C2/c</i> , <i>a</i> = 5.7760(6) Å, <i>b</i> = 9.9859(9) Å, <i>c</i> = 11.1573(11) Å, β = 99.606(4)°, <i>R</i> _{wp} = 4.27%, <i>R</i> _e = 3.31%, <i>R</i> ₁ = 1.46%						
Na1	4d	1/4	1/4	1/2	0.56(8)	
Na2	8f	0.221(2)	0.4125(11)	−0.004(2)	0.56	
Na3/Tb1	4e	0	0.746(3)	1/4	0.56	0.80(3)/0.20
Na4/Tb2	4e	0	0.4197(14)	1/4	0.56	0.20/0.80
Tb3	4e	0	0.0842(13)	1/4	0.56	
O1	8f	0.1559(13)	0.5624(9)	0.1454(9)	0.55(7)	
O2	8f	0.1043(11)	0.2510(15)	0.1432(6)	0.55	
O3	8f	0.1374(15)	0.9247(10)	0.1414(9)	0.55	
<i>T</i> = 2.6 K						
Space group <i>C2/c</i> , <i>a</i> = 5.7671(8) Å, <i>b</i> = 9.9653(10) Å, <i>c</i> = 11.1249(11) Å, β = 99.700(9)°, <i>R</i> _{wp} = 9.39%, <i>R</i> _e = 3.31%, <i>R</i> ₁ (crystal) = 1.81%, <i>R</i> ₁ (magnetic) = 1.95%, μ _{Tb} = 6.04(7) μ _B .						
Na1	4a	1/4	1/4	1/2	0.1(1)	
Na2	8f	0.223(2)	0.4111(18)	0.0039(16)	0.1	
Na3/Tb1	4e	0	0.7321(18)	1/4	0.1	0.80/0.20
Na4/Tb2	4e	0	0.4234(5)	1/4	0.1	0.20/0.80
Tb3	4e	0	0.0866(7)	1/4	0.1	
O1	8f	0.154(2)	0.5709(18)	0.1454(15)	0.2(1)	
O2	8f	0.1025(15)	0.2563(19)	0.1411(10)	0.2	
O3	8f	0.141(2)	0.9327(15)	0.1421(14)	0.2	

Table 2. Structural parameters for Na₂CeO₃ determined by the x-ray diffraction measurement at room temperature. (Note: space group *C2/c* (No 15); *Z* = 8. *a* = 6.0068(9) Å, *b* = 10.383(1) Å, *c* = 11.793(2) Å, β = 110.17(1)°, *R*_{wp} = 14.69%, *R*_e = 6.24%, *R*₁ = 3.98%.)

Atom	Site	<i>x</i>	<i>y</i>	<i>z</i>	<i>B</i> (Å ²)	Occupancy
Na1	4a	0	0	0	0.27(4)	
Na2	8f	−0.041(2)	0.326(1)	−0.006(1)	0.27	
Na3/Ce1	4e	0	0.8369(9)	1/4	0.27	0.65(1)/0.35
Na4/Ce2	4e	0	0.1750(6)	1/4	0.27	0.35/0.65
Ce3	4e	0	0.5008(5)	1/4	0.27	
O1	8f	0.232(3)	0.503(3)	0.141(2)	1.0(1)	
O2	8f	0.267(4)	0.135(2)	0.152(2)	1.0	
O3	8f	0.284(4)	0.857(3)	0.130(2)	1.0	

the arrangement of the Tb ions is regarded as the honeycomb lattice. Thus, we have fitted the observed magnetic susceptibility using a high temperature series (HTS) expansion of the honeycomb lattice for the Heisenberg model:

$$\chi_M = \frac{N_A g^2 \mu_B^2 S(S+1)}{3k_B T} \sum a_n (J/k_B T)^n \quad (1)$$

where N_A , g , μ_B , k_B , and J are the Avogadro number, g factor (=2.0), Bohr magneton, Boltzmann constant, and exchange integral, respectively. We used the coefficients a_n ($n = 1-8$) given in previous results [17–19]. The fitting equation was obtained by applying the Padé approximation ([4, 4] Padé) to the equation (1). The calculated susceptibility is shown as

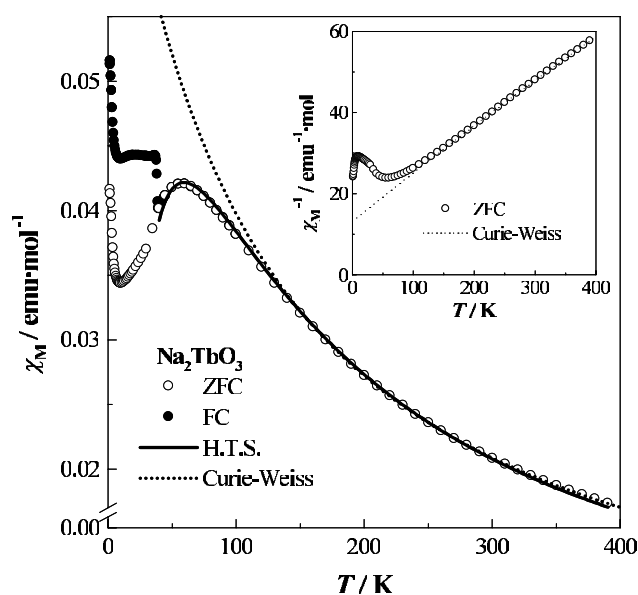


Figure 3. Temperature dependence of the magnetic susceptibility for Na_2TbO_3 . The inset shows the temperature dependence of the inverse magnetic susceptibility.

Table 3. Some selected bond lengths for Na_2TbO_3 at 290 K.

		Na3/Tb1–O1	2.426(23) Å
Na1–O1	2.594(10) Å	Na3/Tb1–O2	2.396(6) Å
Na1–O2	2.377(6) Å	Na3/Tb1–O3	2.367(23) Å
Na1–O3	2.510(10) Å	Average	2.396(18) Å
Average	2.494(8) Å		
		Na4/Tb2–O1	2.135(12) Å
Na2–O1	2.253(17) Å	Na4/Tb2–O2	2.204(18) Å
Na2–O1'	2.521(20) Å	Na4/Tb2–O3	2.238(9) Å
Na2–O2	2.412(19) Å	Average	2.192(13) Å
Na2–O2'	2.633(16) Å		
Na2–O3	2.527(14) Å	Tb3–O1	2.142(10) Å
Na2–O3'	2.634(16) Å	Tb3–O2	2.191(16) Å
Average	2.496(17) Å	Tb3–O3	2.225(13) Å
		Average	2.186(13) Å

a solid line in figure 3, and it is in fairly good agreement with the experimental data. The exchange integral is determined as $J = -2.62(1)$ K.

In addition, this compound shows a sharp increasing of the FC magnetic susceptibility and the divergence between the ZFC and FC susceptibilities at 38.3 K. Our measurements for the magnetization versus magnetic field below T_N show no hysteresis loop; thus the origin of the divergence may be the magnetic frustration of the triangular array of Tb ions, which is locally formed by the partial disordered arrangement. With this disorder, magnetically isolated Tb ions should also exist. Their paramagnetic behaviour may account for the rapid increasing of susceptibilities observed below 5 K.

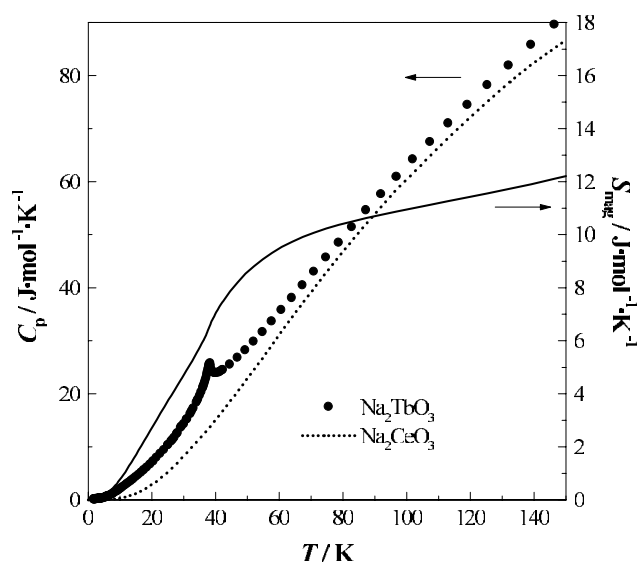


Figure 4. Temperature dependence of the specific heat and magnetic entropy for Na₂TbO₃. The dotted curve represents the specific heat of the nonmagnetic Na₂CeO₃.

3.3. Specific heat

In order to elucidate the origin of the magnetic anomaly at 38.3 K, the temperature dependence of the specific heat for Na₂TbO₃ was measured. It is plotted in figure 4. A λ -type anomaly is observed at the same temperature; this result indicates that the long range antiferromagnetic ordering of Tb⁴⁺ ions occurs. The magnetic entropy change (ΔS_{mag}) associated with this magnetic transition was calculated using $\Delta S_{\text{mag}} = \int (C_{\text{mag}}/T) dT$, in which the magnetic specific heat (C_{mag}) was estimated by subtracting the lattice and electronic specific heat from the experimental specific heat of Na₂TbO₃. For the lattice and electronic contributions, we used the specific heat of a nonmagnetic compound Na₂CeO₃, the structure of which is almost the same as that of the Na₂TbO₃. The temperature dependence of the magnetic specific heat and magnetic entropy is shown in figure 4(b). The magnetic entropy change is 6.6 J mol⁻¹ K⁻¹ at $T_N = 38.3$ K. It is still increasing with temperature and reaches 12.2 J mol⁻¹ K⁻¹ at 150 K. The entropy change is much lower than that expected from the eightfold-degenerate ground state of 4f⁷ ion ($R \ln 8 = 17.32$ J mol⁻¹ K⁻¹). We consider that this is due to two structural features of Na₂TbO₃. One is its 2D character: the short range magnetic ordering in the 2D layer containing Tb ions may begin at a higher temperature than T_N ; actually, the magnetic susceptibility shows a deviation from the Curie–Weiss curve far above T_N . Another is the cation-disorder arrangement. Both the magnetic frustration of the local triangular lattice and the existence of the paramagnetic moment of isolated Tb ions should have decreased the magnetic entropy change.

3.4. Magnetic structure

The powder neutron diffraction profiles for Na₂TbO₃ at 50 and 2.6 K are shown in figures 1(b) and (c), respectively. In the profile at 2.6 K, some additional reflection peaks were found at lower angles, which were not observed at 290 K. All the magnetic peaks can be indexed in the crystallographic unit cell. The data at 50 K show a broad background peak around $2\theta \sim 22^\circ$, which indicates that the onset of the magnetic ordering occurs above T_N .

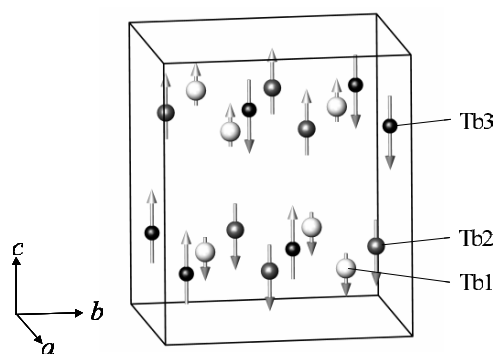


Figure 5. The magnetic structure of Na_2TbO_3 . The arrows represent the direction of the magnetic moment for Tb^{4+} ions, and their lengths reflect the difference in occupation of Tb ions: 20% for Tb1, 80% for Tb2, and 100% for Tb3.

In order to determine the magnetic structure, we assumed that the ordered magnetic moments of the Tb ions at the three sets of 4e sites have the same size and adopt a collinear structure. The magnetic structure determined is illustrated in figure 5, and the structural parameters are listed in table 1. In this magnetic structure, the magnetic moments of Tb ions order antiferromagnetically in each 4e site, i.e., antiparallel, between atomic positions with $z = 1/4$ and $3/4$. The moments of the Tb^{4+} in the Tb1 and Tb2 sites are antiparallel to those in the Tb3 site in the xy layer. The direction of the magnetic moments is parallel to the c axis. The ordered magnetic moment of Tb^{4+} is $6.04(7) \mu_{\text{B}}$, which is slightly smaller than the $7 \mu_{\text{B}}$ expected from the $4f^7$ electronic configuration. This may be due to the influence of the cation disorder as described above.

4. Summary

The crystal structure and magnetic properties for the Na_2TbO_3 containing the Tb^{4+} ion have been investigated. The sample prepared in this study has a 20% disorder of Na and Tb ions in the two 4e sites. From the result of the magnetic susceptibility measurement, magnetic behaviour reflecting a two-dimensional array of Tb ions was observed. This compound also shows the antiferromagnetic transition at 38.3 K, which is exceptionally high like that for the 4f magnet. This magnetic transition is due to the long range ordering of Tb^{4+} ions. The influence of the cation disorder appears in all the magnetic measurements.

Acknowledgments

This research was partially supported by the Ministry of Education, Culture, Sports, Science and Technology, Grant-in-Aid for Young Scientists, No 16750043. This work was also supported by a Grant-in-aid for Scientific Research on Priority Areas ‘Panoscopic Assembling and High Ordered Functions for Rare Earth Materials’ No 17042003 from the Ministry of Education, Science, Sports, and Culture of Japan.

References

- [1] Ramirez A P, Hayashi A, Cava R J, Siddharthan R and Shastry B S 1999 *Nature* **399** 333–5
- [2] Matsuhira K, Hinatsu Y, Tenya K and Sakakibara T 2000 *J. Phys.: Condens. Matter* **12** L649–56

-
- [3] Greedan J E 2001 *J. Mater. Chem.* **11** 37–53
- [4] Ramirez A P 1994 *Annu. Rev. Mater. Sci.* **24** 453–80
- [5] de Jongh L J (ed) 1989 *Magnetic Properties of Layered Transition Metal Compounds* (Dordrecht: Kluwer–Academic)
- [6] Wijn H P J 1997 *Binary Lanthanide Oxides (Landolt–Börnstein New Series vol III/27c1)* (Berlin: Springer)
- [7] Mauger A and Godart C 1986 *Phys. Rep.* **141** 51–176
- [8] Tezuka K, Hinatsu Y, Shimojo Y and Morii Y 1998 *J. Phys.: Condens. Matter* **10** 11703–12
- [9] Hoppe R and Voigt S 1991 Polynary alkali-metal lanthanide oxides *Synthesis of Lanthanide and Actinide Compounds* ed G Meyer and R Moss (Dordrecht: Kluwer–Academic) pp 225–35
- [10] Wolf R and Hoppe R 1988 *Z. Anorg. Allg. Chem.* **556** 97–108
- [11] Zintl E and Morawietz W 1988 *Z. Anorg. Allg. Chem.* **245** 26–31
- [12] Hinatsu Y and Doi Y 2005 to be submitted
- [13] Hoppe R and Seeger K 1968 *Naturwissenschaften* **55** 297
- [14] Ohoyama K, Kanouchi T, Nemoto K, Ohashi M, Kajitani T and Yamaguchi Y 1998 *Japan. J. Appl. Phys.* **37** 3319–26
- [15] Izumi F and Ikeda T 2000 *Mater. Sci. Forum* **321–324** 198–203
- [16] Shannon R D 1976 *Acta Crystallogr. A* **32** 751–67
- [17] Rushbrooke G S and Wood P J 1958 *Mol. Phys.* **1** 257–83
- [18] Stephenson R L, Pirmie K, Wood P J and Eve J 1968 *Phys. Lett. A* **27** 2–3
- [19] Yamaji K and Kondo J 1973 *J. Phys. Soc. Japan* **35** 25–32